# A Wideband Balun — How Does it Work?

Antennas often require a balanced feed system like the circuit described in this article

**By J. Thaysen, K. B. Jakobsen and J. Appel-Hansen**
Technical University of Denmark

Whenever a balanced antenna (i.e., dipole, loop or spiral) is used, the issue of how to feed the antenna becomes relevant. Because a balanced antenna requires a balanced feed, a balun is needed.

A balanced antenna fed by a two-wire transmission line is a balanced system with respect to the lines, provided that the two feed points on the balanced



▲ **Figure 1. Balun for use with a spiral antenna.**

antenna have the same orientation and placement with respect to the lines. If the balanced (symmetrical) antenna is connected to a coaxial transmission line, the transition from the feed line to the balanced antenna is an unbalanced (asymmetrical) driven system. The balun is inserted between the feed line and the antenna in order to provide a transition between the coplanar waveguide (CPW) and the coplanar strip line (CPS). The balun produces a symmetrical radiation pattern however, this article does not deal with the radiation from a connected antenna.

In some applications, it is necessary to connect the feed terminals on the balanced antennas to an unbalanced coaxial cable that requires not only a balanced-to-unbalanced transformation circuit, but also an impedance match due to the different characteristic impedances of the antenna and the cable.

In the literature, different types of baluns are described [1, 2]. In this article, the focus is solely on a planar balun [3] because it has some very good qualities, such as a low insertion loss and wide bandwidth. The balun is planar, which
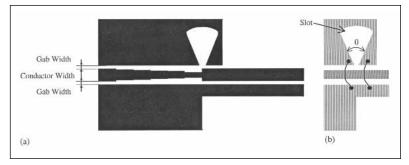
makes it realizable using conventional photo techniques.

To aid the balun design and characterization, the electromagnetic simulation program IE3D Version 6.03, a method of moment computer program developed by Zeland Software [4], was used to predict the performance of the balun structure. The measured results of the constructed balun structure were then compared to the simulated results obtained from IE3D.

Baluns whose characteristics remain virtually unchanged over an exceptionally large bandwidth have a multitude of uses. For example, they can be used for ground penetrating radar where the use of a wideband antenna is necessary [5, 6].

## The principle of the balun

The wideband coplanar-waveguide to coplanar-stripline (CPW-to-CPS) balun was designed to transform the unbalanced CPW feed line to a balanced CPS feed line. The balun shown in Figure 1 is intended to be used with a spiral antenna. The CPW-to-CPS balun is a modified version of Li's [7], and a somewhat similar

balun configuration was successfully used in [8]. To characterize the balun, a model of the structure is shown in Figure 2. This model is used to explain the different parts of the balun.

*Coplanar waveguide (a)* — Due to the difference in the impedance between the two-arm spiral antenna and the unbalanced coaxial cable feedline, it is necessary to provide an impedance match as well as balanced-to-unbalanced transformation.

The impedance match between the cable and the balun is obtained by using a Chebyshev multi-section impedance transformer circuit. Depending on the ratio between the two impedances, the number of sections can be numbered. In this case, a four section Chebyshev impedance transformer with a reflection coefficient of $\Gamma_m = 0.05$ was designed to transform the impedance from 50 ohms to 80 ohms.

*Balun (b)* — The actual transformation between the unbalanced and the balanced mode is achieved by the balun. The coplanar waveguide (a) and the coplanar strip line (c) are only needed to connect the sender/receiver and the antenna.

The balun is quite complex by itself. The basis of it is the wideband transition from the CPW-to-CPS, which is accomplished through a radial slot. This slot represents a very wideband open circuit, which forces the electrical field to be mainly between the two conductors of the CPS, as illustrated in Figure 8. The two bond wires near the discontinuity plane ensure that the potential on the two ground planes is equal, as shown in Figure 1(b).

*Coplanar strip line (c)* — The balanced output from the balun is connected to the antenna using the balanced coplanar strip line. The distance between the balun and the antenna determines the length of the strip line. Because a short distance is preferred, the balun is placed as close to the antenna as possible.

*Transmission line model of the balun circuit* — A transmission line model of the entire balun structure, including a four section Chebyshev section impedance transformer, is shown in Figure 3.

### Balun configuration

Choosing a substrate is a bottleneck when designing the CPW and CPS, because both the CPW and the CPS have to be designed on the same substrate and have the same impedance, namely $Z_{ANTENNA}$. Using classic equations for CPW and CPS [2], it is found to be feasible to use a substrate material having a relative permittivity of 10.2 and a thickness of 0.785 mm. These parameters are chosen as a trade-off between the permittivity and the thickness, so that standard substrate parameters can be used.

The next step involves the design of the impedance transformer, which is accomplished using the classic
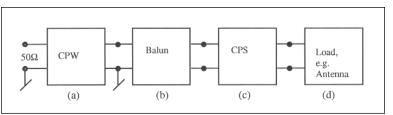


▲ **Figure 2. Balun consisting of a coplanar waveguide (a); balun (b); coplanar strip line (c); and the coplanar strip line connected to a balanced antenna (d).**
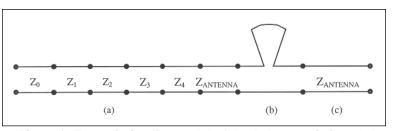


▲ **Figure 3. Transmission line model of the balun consisting of the coplanar step impedance waveguide (a), the balun (b), and the coplanar strip line.**

equations for Chebyshev multi-section matching transformers [9] when deciding how many sections the transformer should have.

Preliminary simulations found that the length of the ground plane is proportional to the upper usable frequency of the balun. Also, an inverse proportionality was found between the length of the sections in the impedance transformer and the reflection coefficient ($S_{11}$). Choosing the number and the length of the sections is therefore a trade-off between a high bandwidth and a low reflection coefficient. To optimize the balun with respect to the bandwidth, it is necessary to reduce the overall length of the balun. By choosing four sections, each is minimized to 3 mm.

The design impedance is found by using the equations for the CPW and the CPS. Next, the physical dimensions are found and are adjusted with respect to production tolerances. The adjusted results are then used to calculate the impedance with the use of IE3D.

The width of the ground plane of the CPW is 15 mm, due to symmetry. It is, however, desirable to minimize the overall size of the structure, resulting in a cheaper and smaller solution. Thus, simulations are carried out in order to decrease the width of the CPW.

By changing the width of the CPW from 15 mm to 6.5 mm, the balun is optimized with respect to the bandwidth — that is, the upper frequency for a reflection coefficient higher than 10 dB is increased 20 percent. In [4], it was found that the optimal width for the ground plane of the CPW is about 2.5 times the distance between the two ground planes, which is in accordance with the results presented in Table 1.

| Four-section Chebyshev step impedance transformer having an impedance ratio $Z_0/Z_L = 80/50 = 1.6$ | CPW | | | | | | CPS |
|---|---|---|---|---|---|---|---|
| | $Z_0$ | $Z_1$ | $Z_2$ | $Z_3$ | $Z_4$ | $Z_{ANTENNA}$ | $Z_{ANTENNA}$ |
| Design impedance [Ω] | 50 | 55.4 | 60.5 | 66.7 | 72.6 | 80 | 80 |
| The physical parameters are adjusted with respect to production tolerance   Strip width [mm]   Gab width [mm]   Length of the sections [mm] | 1.7 0.45 3 | 1.5 0.55 3 | 1.3 0.65 3 | 1.1 0.75 3 | 0.9 0.85 3 | 0.7 0.95 30 | 1.8 0.4 |
| Calculated impedance of the adjusted parameters using IE3D [Ω] | 49.8 | 54.4 | 59.4 | 64.7 | 71.6 | 79 | 81 |

▲ **Table 1. Calculated results for the four sections Chebyshev step impedance transformer.**

Simulations with and without bond wires are performed. To ensure proper operation of the balun, it is necessary to state that the two bond wires are located near the discontinuity plane. The simulated as well as the prototyped bond wires have a diameter of 0.15 mm.

With the bond wires, the bandwidth for a reflection coefficient better than –10 dB of the balun is 0.1 to 3.45 GHz, whereas the bandwidth for the balun without any bond wires is as low as 0.1 to 0.5 GHz and from 1.95 to 2.4 GHz. From 0.5 to 1.95 GHz and 1.95 to 3.45 GHz, the reflection coefficient is simulated to be below –5 dB, as shown in Table 2. In conclusion, we find that the bond wires have to be used. This result has been verified through measurement.

Recently, a description of a balun was published based on the same principle, except that it did not benefit from a radial slot [10]. That balun is rather narrow-banded compared with the balun discussed in this article.

The advantages of a radial slot over a rectangular slot are smaller resonance length and wider bandwidth [11]. Based on experimental investigation, it is found that the optimized angle, θ, of the radial slot is 45 degrees [5]. In this article, the simulated dimensions of the radial slot are a radius of 6 mm and an angle of 45 degrees [12].

Kolsrud, et al. [13] argue that a balun with a circular slot provides a larger bandwidth compared to a balun with a radial slot. Two back-to-back balun structures (one having radial slots, the other circular slots) were simulated and prototyped in order to find the most broadband configuration. The simulated as well as the measured results for the back-to-back coupled balun are shown in Table 2.

The simulated upper frequency for a reflec-

tion coefficient higher than –10 dB is 3.6 and 3.45 GHz for the balun structure with circular and radial slots, respectively. The measured upper frequency for a reflection coefficient higher than –10 dB is 3.3 and 3.4 GHz for the balun structure with circular and radial slots, respectively. The balun with the radial slot yields the best solution because of a somewhat lower insertion loss and a better reflection coefficient though the band of operation frequencies.

The simulations carried out are not exhaustive and it is possible that different results can be obtained by changing some parameters.

## Numerical and experimental results

To analyze the balun, IE3D was used to simulate the performance of the printed balun in terms of the $s$-parameters, as well as the current distribution on the metallic surface of the balun structure. Twenty cells per wavelength and edge cells are used to model the balun structure [4].

The balun structure shown in Figure 4 was fabricated on a Rogers RT/Duroid® substrate with a thickness of 0.785 mm and a relative dielectric constant $\varepsilon_r$ of 10.2.

Two back-to-back CPW-to-CPS transitions were simulated and optimized using IE3D. The baluns were connected so that the unbalanced port of each balun was accessible externally. The SMA connectors and the wire bonding were soldered directly on the substrate. The

| | Frequency range with a return loss better than 10 dB | | | |
|---|---|---|---|---|
| | Bandwidth for $S_{11} < -10$ dB [GHz] | | Insertion loss for $S_{11} < -10$ dB [dB] | |
| | Simulated | Measured | Simulated | Measured |
| Without bondwires, with radial slot | 0.1–0.9 | 300 kHz–0.75 | < 1 | < 1 |
| With bondwires, without slot | 0.1–2.5 | | | |
| With bondwires, with circular slot | 0.1–3.6 | 300 kHz–3.3 | < 1.3 | < 2.5 |
| With bondwires, with radial slot | 0.1–3.45 | 300 kHz–3.4 | < 1 | < 2 |

▲ **Table 2. Measured and simulated results for the back-to-back coupled balun.**

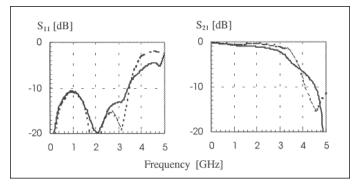▲ **Figure 4. Back-to-back coupled balun placed on RT/Duroid substrate.**



▲ **Figure 5. Measured (solid) and simulated (dashed) S-parameters for the two baluns mounted back-to-back.**
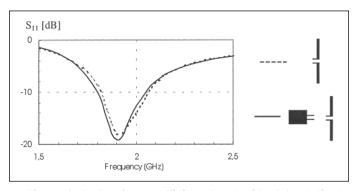


▲ **Figure 6. Reflection coefficient for the ideal feed dipole antenna (dotted) and for the dipole feed via the simulated balun (solid).**

size of the prototype is $16 \times 46$ mm. The structure was fabricated to verify the bandwidth and insertion loss. In terms of scattering parameters, the numerical results can be compared with the experimental results in Figure 5. The result for $S_{11}$ seems to be the most accurate; however, the agreement is good for frequencies up to 2.5 GHz. The insertion loss (i.e., the $S_{21}$), the numerical and the experimental result similarities are obtained. The simulated as well as the measured results show an upper frequency limit where the reflection coefficient is 10 dB at 3.4 GHz. Good agreement is obtained between the simulated and measured balun for frequencies up to 4.5 GHz.

The structure was tested on an HP 8720D and an HP 8752A network analyzer to determine the reflection coefficient and the insertion loss of the balun. The two back-to-back CPW-to-CPS transitions provide a measured insertion loss of less than 2 dB from 300 kHz to 3.4 GHz with a reflection coefficient higher than –10 dB. Although the balun characteristics are measured starting from 300 kHz, the lower limit of the frequency bandwidth is nearly DC.

## Test of the balun

Additional simulations of the discussed balun were carried out to verify the validity of the balun and to test the validity of the simulation.

The simulations and the measurements on the constructed prototypes verify the principle for the balun. In order to verify the balun it is necessary to investigate a single balun.
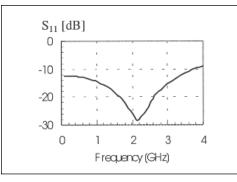
In IE3D, it is possible to merge two individually simulated structures (e.g., a balun concatenated to a dipole antenna). This setup can be made by simulating the balun, then simulating the dipole, and finally merging the two resulting files to end up with the result for the concatenated circuit [4] — for example, the scattering parameters of the dipole feed by the balun.

An ordinary planar half wavelength dipole with a length of 50 mm placed on the same substrate was used for the balun, and is expected to have constant input impedance around the resonant frequency. The planar dipole is a small and simple structure, causing a simulation time of only a few seconds. The simulated reflection coefficient for the planar dipole is shown in Figure 6.

In Figure 6, the comparison of the simulated reflection coefficient for the ideal feed dipole antenna and the simulated reflection coefficient for the dipole feed via the simulated balun shows that there are virtually no differences. In both cases, the resonant frequency is 1.9 GHz and the bandwidth is 250 MHz, for a reflection coefficient higher than –10 dB. The result indicates that the balun actually works as a balun and that IE3D can be used to concatenate two individually simulated structures. It should be noted that the free space resonant frequency for the dipole is 3 GHz, but due to the dielectric loading (substrate), the resonant frequency is lowered to 1.9 GHz only.

The balun is intended to be used as the feed network for a frequency independent antenna (e.g., a spiral antenna). In order to verify how frequency independent the balanced port on the balun are with respect to the input impedance, simulations on the balun using IE3D are performed by terminating the CPS with an ideal 80-ohm resistor. The result is shown in Figure 7.

In the frequency range from 0.1 to 3.85 GHz, the sim-

▲ Figure 7. Simulated reflection coefficient $s_{11}$-parameter for the balun where the CPS is terminated by an ideal 80-ohm resistor.
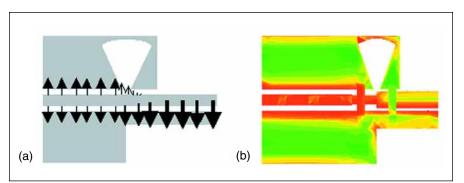


▲ Figure 8. Electrical field pattern for the CPW-to-CPS balun (a). The average current density is shown in (b) where the density at each location is illustrated by IE3D where red indicates the highest and green the lowest current density.

ulated reflection coefficient is better than –10 dB. For the balun loaded with an ideal 80 ohm resistor, the simulated bandwidth within which the reflection coefficient is better than –10 dB is higher than the bandwidth obtained for the back-to-back balun, because of the interaction between the two baluns. The actual balun is used with a spiral antenna, where the measured upper frequency limit is 3.8 GHz for a reflection coefficient better than 10 dB [3].

Simulations are carried out in order to investigate the physical operation of the balun. A sketch of the electrical field pattern is shown in Figure 8. The sketch shows how the slot forces the field to be transformed from a symmetrical pattern between the center conductor and the two ground planes of the CPW to be mainly between the two conductors of the CPS. Furthermore, the average current density, calculated using IE3D, is shown in Figure 8. The figure shows that the highest current densities for the CPW are in the vicinity of the center conductor of the CPW and at the edges on the two ground planes of the CPW. On the CPS, the highest current density is symmetrical in the vicinity of the two conductors' edges.

The arrows shown in Figure 8 indicate the direction and the density of the current at a specific location. The current is flowing from the CPW to the CPS through the ground plane on the CPW to one of the CPS conductors' edges. The current is flowing in the opposite directing (i.e., from the opposite conductor on the CPS via the center conductor of the CPW).

The grid shown in Figure 9 is the result of the automatic grid in IE3D. Near the edges, the modeled structure consists of edge cells which leads to a higher accuracy of the simulated results, compared with the measurements performed on the constructed prototype [4]. Also, this feature yields a 3 to 5 times longer simulating time, which means the user can use it only where high precision of the simulated results is required. For further discussion, see Zeland Software's IE3D [4].

## Conclusions

The use of the electromagnetic simulation program IE3D to verify the theoretically expected performance with a measured prototype has been demonstrated. The scattering parameters can be predicted with good accuracy using the simulator. Howevcr, due to limitations such as infinite dielectric layer and non-homogeneous metal thickness due to the solder and connectors, everything that is measurable cannot easily be simulated. Generally, the simulations offer a fast and reasonably accurate way of investigating the balun structure.

A wideband coplanar waveguide to coplanar strip transition, which covers a frequency range from practi-
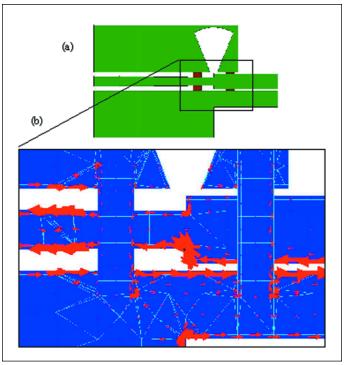


▲ Figure 9. The CPW-to-CPS balun (a). A Close-up picture of the current density where the arrows show the direction and the density of the current at a specific location (b).

cally DC to 3.85 GHz with a reflection coefficient better than –10 dB, was presented. Good agreements were obtained between the numerical results and the measured results in the frequency range from 300 kHz to 5 GHz using an HP 8753 and an HP 8720 network analyzer. IE3D simulations have been used to verify that the balun structure operates as a balun, with the balun structure showing that the input impedance is essentially constant over a bandwidth from 0.1 GHz to 3.85 GHz.

By using a Chebyshev impedance transformer, the balun design allows impedance transformation in addition to providing the necessary transition from the unbalanced feed line (e.g., coaxial cable, microstrip and coplanar waveguide) to the balanced feed line (e.g., coplanar strip line).

The balun described here, which is as small as 16 × 46 × 0.8 mm, is designed and prototyped for the RT/Duroid 6010 substrate having a relative dielectric constant $\varepsilon_r$ of 10.2. Also, the proposed design is uniplanar and thus feasible to realize using ordinary photographic fabrication techniques without the need of additional components, such as a wire wound transformer. However, this article has shown that wire bonding near the discontinuity plane improves the performance of the balun.

The balun has several advantages, including very wide bandwidth, relatively small size and low profile. The balun could easily be integrated as part of a microstrip circuit, which furthermore yields a low-cost solution. Thus, the balun should find many applications in broadband systems. ∎

## References
1. H. Shuhao, "The Balun Family," *Microwave Journal,* Technical notes, Vol. 30, pp. 227–229, 1987.
2. R. C. Johnson, and Jasik, H., *Antenna Engineering Handbook, Third Edition,* McGraw-Hill, 1993.
3. J. Thaysen, K. B. Jakobsen, and J. Appel-Hansen, "Characterisation and optimisation of a coplanar waveguide fed logarithmic spiral antenna," accepted for the IEEE AP-S Conference on Antennas and Propagation for Wireless Communication, Waltham, MA, November 2000.
4. "IE3D User's Manual, Release 6," Zeland Software, Inc., Fremont, CA, 1999.
5. J Thaysen, "Logarithmic spiral antenna and feed network for application to humanitarian demining," Department of Applied Electronics and Department of Electromagnetic Systems, Technical University of Denmark, in Danish, March 2000.
6. J. Thaysen, K.B. Jakobsen, and J. Appel-Hansen, "Ultra wideband coplanar waveguide fed spiral antenna for humanitarian demining," accepted for the IEEE, 30th European Microwave Conference, Paris, France, October 2000.
7. Y.M. Li, K. Tilley, J. McCleary, and K. Chang, "Broadband coplanar waveguide-coplanar strip-fed spiral antenna," *Electronic Letters,* Vol. 30, pp. 176–177, 1995.
8. J. Thaysen, K.B. Jakobsen, and J. Appel-Hansen, "Numerical and experimental investigation of a coplanar wave guide fed spiral antenna," IEEE *The 24th QMS Antenna Symposium,* London, England, April 2000.
9. D.M. Pozar, *Microwave Engineering, Second Edition,* John Wiley & Sons, 1998.
10. Y-D. Lin, S-N. Tsai, "Coplanar waveguide-fed uniplanar bow-tie antenna," *IEEE Transactions on Antennas and Propagation,* Vol. 45, pp. 305–306, 1997.
11. R.N. Simons, S.R. Taub, "Coplanar waveguide radial line stub," *Electronics Letters*, Vol. 29, pp. 412–414.
12. V. Trifunovic, and B. Jokanovic, "Four decade Bandwidth Uniplanar Balun," *Electronics Letters,* Vol. 28, pp. 534–535, 1992.
13. A.T. Kolsrud, M-Y. Li, and K. Chang, "Dual-frequency electronically tunable CPW-fed CPS dipole antenna," *Electronics Letters,* Vol. 34, pp. 609–611, 1998.

## Author information
Jesper Thaysen received his M.Sc.E.E. from the Technical University of Denmark, Lyngby, in 2000. His professional interests include antennas, microwaves, ground penetrating radar and communication. He currently works as an electrical engineer at the Department of Applied Electronics at the Technical University of Denmark. He can be contacted by e-mail: jt@iae.dtu.dk; phone: +45 4525 5263; or fax: +45 4525 5300.

Kaj B. Jakobsen received his M.Sc.E.E. from the Technical University of Denmark, Lyngby, in 1986, and his Ph.D. from the University of Dayton, Dayton, OH, in 1989. His professional interests include microwaves, antennas, electromagnetics and communication. He is currently an Associate Professor at the Department of Applied Electronics (IAE) at the Technical University of Denmark. He can be contacted by e-mail: kbj@iae.dtu.dk; phone: +45 4525 5255; or fax: +45 4525 5300.

Jørgen Appel-Hansen received his M.Sc.E.E. and Ph.D. from the Technical University of Denmark, Lyngby, in 1962 and 1966, respectively. His professional interests include electromagnetics, antennas and anechoic chamber measurements on antennas. He is currently an Associate Professor at the Department of Electromagnetic Systems (EMI) at the Technical University of Denmark. He can be contacted by e-mail: ja-h@emi.dtu.dk; phone: +45 4525 3812; or fax: +45 4593 1634.